THERMODYNAMIC AND REACTIVITY ASPECT OF B-CYCLODEXTRINE INCLUSION COMPLEXES WITH COUMARIN DERIVATIVES

G. BARRIGA – GONZÁLEZ [a] *AND J. MUÑOZ – ESPINOZA* [a] *

[a]*Department of Chemistry, Faculty of Basic Science, Metropolitan University of Education Sciences, Santiago, Chile.*

ABSTRACT

In this study, the thermodynamic and reactivity characteristics of coumarin-derived ligand inclusion complexes with βCD were described, in addition to the *in situ* reactivity of these ligands and their changes in the complex cavity. For this purpose, computational tools such as molecular docking, second order perturbative analysis (E2PERT), ONIOM2 (DFT/PM6) methods were employed to obtain the global and local reactivity indices, and thermodynamic parameters, in addition to non-covalent interaction (NCI) analysis. As a result, it can be observed that the inclusion complexes are stable and viable given the ability to form non-covalent interactions, but their formation is not spontaneous under the modeling conditions. The global and local reactivity indices show that the ligands change their chemical reactivity inside the inclusion complex, demonstrating that the studied ligands present AOX SET activity outside the cavity, and HAT activity inside the cavity, mainly the C1 and C3 ligands.

Keywords: Docking, Coumarin, β-Cyclodextrin, Reactivity, Thermodynamic.

1. INTRODUCTION

Coumarins (1,2-benzopyrone) are organic compounds belonging to the Lactone family, which are widely distributed in nature as they are secondary metabolites of phenylalanine in metabolic processes in plants, fungi and bacteria [1]. They present diverse functions in the fields of chemistry and biology, since they are versatile and easily modified through the addition of substituents such as phenolic groups and heterocyclic rings. Given their versatility, coumarins present anti-inflammatory [2], anticoagulant [3], antiviral [4], and antioxidant capacities, as established by Pérez-Cruz et. al [5] in their study of antioxidant capacity on the trypanocidal activity (Chagas disease generated by the T. Cruzi parasite) of a series of 4-hydroxycoumarin derivatives.

Cyclodextrins (CDs) are cyclic macromolecules derived from starch that are made up of α-1,4-D-glucopyranose units, and given the conformation of the glucopyranose units, this molecule presents an asymmetric toroidal structure with a hydrophobic cavity and a hydrophilic external face due to the arrangement of the hydroxyl groups that are oriented towards the external face of the macromolecule [6,7]. Given the characteristics of internal hydrophobicity and external hydrophilicity, cyclodextrins are potential candidates for the transport and modification of physicochemical characteristics of molecules forming host-guest inclusion complexes [8].

The ability of inclusion complex formation is mainly due to the thermodynamics of the process [9] and possible non-covalent interactions (NCI) between the ligand and the CD cavity [10]. Thermodynamically, the inclusion process is guided by the inclusion constant (K_i), entropy (ΔS), enthalpy (ΔH), and Gibbs free energy of reaction (ΔG) [11,12,13], in addition to the non-covalent interactions between the ligand and the cavity [10,14]. In turn, the stability of the inclusion complex can be described from the interaction energy (ΔE_{int}) by considering the *Basis Set Superposition Error* (BSSE), which is a phenomenon associated with the interaction and superposition of basis functions of interacting molecular systems [11,15,16].

The non-covalent interactions that are generated between the ligands and the βCD cavity can be modeled and described through a second-order perturbative analysis (E2PERT) [17,18] which describes the interactions between Lewis (donor) and Non-Lewis (acceptor) type natural bond orbitals (NBO) [19] of the βCD/coumarin system, in addition to an electron density mapping that allows describing the types of non-covalent interactions [20].The main antioxidant mechanisms (AOX) are SET mechanisms (one electron transfer mechanism) which is described as the ability to neutralize a free radical when it yields an electron to an electroacceptor species, mainly molecular species presenting rings with resonant π electrons [21], and HAT mechanisms (one hydrogen atom transfer) which neutralizes free radicals when it yields labile hydrogens from a homolytic radical cleavage [22]. The SET and HAT mechanisms are related to the global and local reactivity indices, the SET mechanism being described by the chemical potential (μ) [23] and the Electrophilicity (ω) [24,25,26], while the HAT mechanism is described by the Fukui functions ($f_{(r)}$) [27] and the Dual Descriptor ($f^{(2)}$) [28]

The present study aims to model and describe the chemical reactivity of a series of coumarin derivatives and how they form inclusion complexes with β-Cyclodextrin.

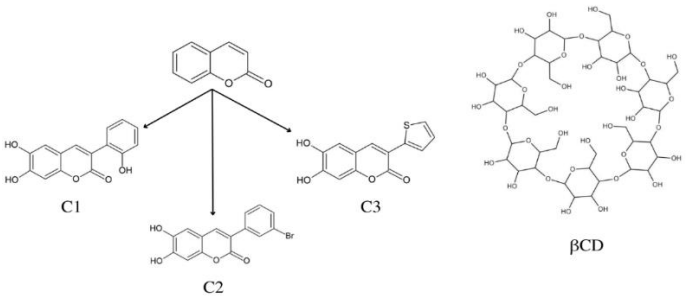

Figure 1. Coumarin (1,2-benzopyrone), its derivatives and β-Cyclodextrin.

2. COMPUTATIONAL DETAILS

2.1 Ligand and β-Cyclodextrin optimization

For the design and construction of coumarin-derived ligands, GaussView 5.0.9 software was used, while geometrical optimizations were performed in Gaussian '09 revision E.01 [29], using the Density Functional Theory (DFT) method with the WB97XD/6-31G+(d,p) functional, which is long-range corrected functional possessing satisfactory yields for modeling non-covalent interactions (NCI) [30].

For its part, β-Cyclodextrin was obtained from the crystal structure of the β-amylase/β-cyclodextrin complex [31] from the Protein Data Bank database under the code 1BFN, optimizing its structure in the same way as coumarin ligands.

2.2 Molecular docking

The βCD/coumarin inclusion complex was carried out using Autodock 4.2 software, in which a blind Docking (in gas phase and at a pressure of 1 atm and temperature of 298 K) was carried in order to find a possible more stable conformation of inclusion of the ligand inside the cavity [32]. The conformational search site was delimited in a box with dimensions $x = -7{,}25$ Å, $y = 28{,}35$ Å, $z = 29{,}56$ Å and a grid resolution of 0,375 Å. The ligand docking method was of the semi-flexible type, i.e. the βCD presented a rigid structure, while the ligands were flexible, the ligands being in charge of rotating and moving in the cavity until finding a conformational space of lower energy. The criterion for choosing the optimal conformer was the minimum coupling energy [33].

*Corresponding author email: jose.munoz2017@umce.cl

2.3 Second-order perturbation analysis (E2PERT)

For obtaining the second-order perturbative parameter (E2PERT) and the interactions between Lewis-type (donor) and non-Lewis-type (acceptor) orbitals, between ligands and the βCD cavity, the ONIOM2 method [34] with DFT (*high*) and semiempirical PM6 (*low*) theory levels were considered. The E2PERT calculation was carried out in NBO 6.0 software [35].

2.4 Thermodynamic parameters

To obtain the interaction energy of the inclusion complex, a DFT level of theory was used with the Counterpoise correction tool which considers the basis set superposition error (BSSE). On the other hand, to obtain the thermodynamic parameters of the ligands, βCD and inclusion complexes in gas phase, their associated frequencies were calculated with a Semiempirical PM6 level of theory [36].

2.5 Non Covalent Interactions (NCI)

To model the non-covalent interactions generated in the βCD/ligand system, the Multiwfn 3.7 software was used, which through the electronic information (molecular wave function) can generate an electron density map that allows describing the types of non-covalent interactions [20]. The graphical analysis of the NCI generates a high-resolution grid consisting of 17.2 million points surrounding the entire molecular system, which can be visualized in the software VMD 1.9.4.a51 which is a visualizer of molecular structures and dynamic simulations [37].

2.6 Local and global reactivity indices of ligands and inclusion complexes

Local and global reactivity indices of ligands were obtained via Fukui 4.1 software [38,39,28] compatible with Gaussian '09. The calculation was performed through a *singlepoint* (SP) in Gaussian '09, and its output file was read in Fukui 4.1.

For its part, the reactivity indices of the inclusion complexes, the ONIOM2 method [34] was used for which two levels of theory (DFT/PM6) were considered. In the same way, the output file was read in Fukui 4.1 software.

To plot the local descriptors (Fukui and dual descriptor), the Fukui boundary molecular orbitals approximation [35] was used, which were visualized in GaussView generating isosurfaces of density 0,002 u. a.

3. RESULTS AND DISCUSSION

3.1 Optimized Structures and Inclusion Complexes

The ligands derived from Coumarin and β-Cyclodextrin modeled and optimized with the DFT level of theory and the long-range hybrid functional WB97XD/6-31G+(d,p) can be visualized in Figure 2.

Although the ligands were optimized prior to the formation of the inclusion complex, it can be observed (Figure 3) that after molecular docking, rotations of the hydroxyl groups and rings are evident, which is caused by the flexibility of the ligand and the rigidity of the cavity to find a lower energy conformation [40,41].

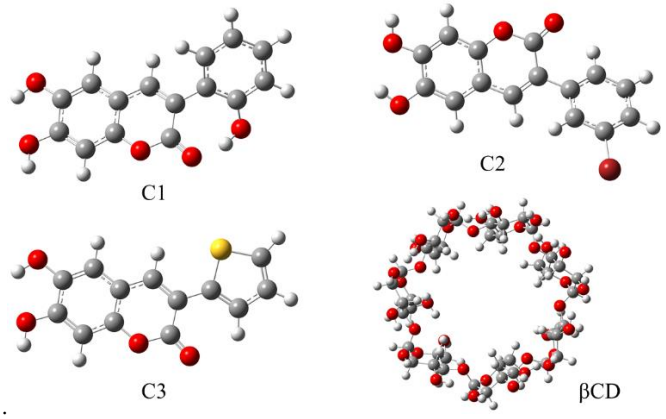

Figure 2. Coumarin derived ligands and β-Cyclodextrin optimized.

As a result of blind molecular docking between coumarin and βCD derivatives it can be observed that the ligands present different spatial arrangement within the cavity, since the C1 and C3 ligand present immersed *a* and *b* rings towards the position of the primary hydroxyls, while the C2 ligand places its *a* and *b* rings towards the secondary hydroxyls, with the *c* ring remaining within the cavity.

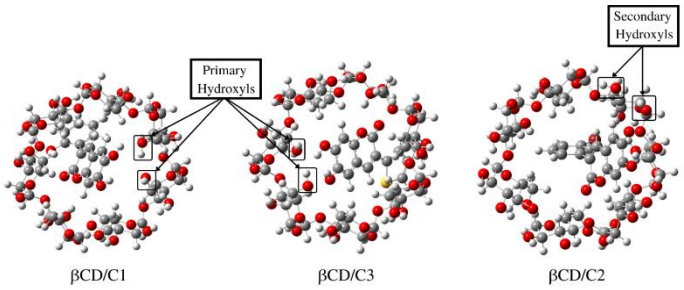

Figure 3. Coumarin-derived inclusion complexes and βCD generated by molecular docking.

Although the modeling of inclusion complexes by molecular docking is of great utility to obtain blind conformational spaces when no experimental information is presented, it also presents certain limitations that could depart from the real phenomenon of complexation. One of these limitations is the reaction stoichiometry, i.e., the amount of ligands interacting per unit βCD, and vice versa, the amount of βCD acting per unit ligand. Since complexation is guided by steric effects (cavity volume and ligand size), depending on the ligand size a 1:1 or 1:2 inclusion complex can be generated, or a large ligand can be surrounded by more than one βCD [42].

Another limitation of molecular docking is the kinetic and thermodynamic description of the process, since inclusion processes are mainly guided by the inclusion constant (K_i) and the Gibbs free energy of reaction (ΔG) [11]. A last limitation is the solvent effect [11,43] which is a parameter of utmost importance in the stability of the complex, since one of the objectives of the study of inclusion complexes is to understand the mechanism of encapsulation of ligands in the βCD cavity, and how these are stabilized inside through non-covalent interactions of the hydrophobic type and hydrogen bridges in aqueous media [44], which cannot be modeled in molecular docking, since a solvation layer inside and outside the βCD is not considered, so the thermodynamic results would be far from the experimental results, since it has been observed that when the ligand is encapsulated, it displaces the water molecules from the cavity (desolvation) increasing the entropy of the process, favoring its spontaneity [45,46].

3.2 Second-order perturbation analysis (E2PERT)

A second-order perturbative analysis is a numerical description of the stabilization phenomenon between donor (bonding) orbitals and acceptor (anti-bonding) orbitals of a molecule [19], so in an inclusion complex it can be described as a stability criterion given the interactions of electron densities between the ligand and the βCD [36]. Mathematically, the second-order perturbative analysis is of the form ($E_{ij}^{(2)}$):

$$E_{\phi\phi^*}^{(2)} = -2\frac{\langle\phi|\boldsymbol{F}|\phi^*\rangle^2}{\varepsilon_{\phi^*} - \varepsilon_{\phi}} \quad (1)$$

$\boldsymbol{F}$ being the Fock operator, the natural bonding orbitals (NBO) bonding and anti-bonding, and $\varepsilon_{\phi^*}, \varepsilon_{\phi}$ the energies of the bonding and anti-bonding orbitals [18]. Table 1 shows the donor-acceptor pairs between the ligand and the cavity, and vice versa.

Table. 1. Second-order perturbative analysis (E2PERT) (**notation**: LP: non-bonding electron pairs, BD: bonding orbital, BD*: anti-bonding orbital).

Complex	Donor	Acceptor	$E^{(2)}$ / $(kcal/mol)$
βCD → C1	LP(1) O22	BD*(1) O167 – H168	2,11
	LP(2) O22	BD*(1) O167 – H168	1,47
	BD(1) C49 – H122	BD*(1) C160 – H177	2,36
	BD(1) C39 – H113	BD*(1) C160 – H170	1,93
	BD(1) C58 – H130	BD*(1) O169 – H170	2,11
	BD(1) O22 – H97	BD*(1) O167 – H168	1,70
	BD(1) C17 – O22	BD*(1) O167 – H168	1,26
C1 → βCD	BD(2) C151 – C152	BD*(1) C69 – H140	2,39
	BD(1) C155 – H175	BD* C5 – H82	1,35
	BD(1) C160 – H177	BD*(1) C38 – H113	2,77
	BD(1) 160 – H177	BD*(1) C49 – H122	2,03
	BD(2) C161 – O162	BD*(1) C56 – C130	2,40
	BD(1) O167 – H168	BD*(1) O22 – H97	1,10
βCD → C2	BD(1) O29 – H105	BD*(1) O167 – H168	2,27
	BD(1) C25 – H100	BD*(1) C158 – H175	8,11
	BD(1) C49 – H122	BD*(1) C148 – H169	1,54
C2 → βCD	LP(1) O159	BD*(1) C3 – H80	1,16
	BD(1) C148 – H169	BD*(1) C49 – H122	2,41
	BD(2) C156 – C157	BD*(1) C14 – H90	1,73
	BD(1) C158 – H175	BD*(1) C25 – H100	7,91
	BD(2) C161 – O162	BD*(1) C5 – H82	3,17
βCD → C3	LP(2) O22	BD*(1) O166 – H167	2,58
	LP(2) O33	BD*(1) O164 – H165	2,10
	BD(1) C5 – H82	BD*(1) C157 – H172	2,52
	BD(1) O22 – H97	BD*(1) O166 – H167	1,64
	BD(1) C38 – H112	BD*(1) C159 – H173	1,26
C3 → βCD	LP(2) O166	BD*(1) C16 – H92	1,44
	BD(1) C154 – H171	BD*(1) C69 – H140	1,96
	BD(1) C157 – H172	BD*(1) C5 – H82	3,04
	BD(1) C159 – H173	BD*(1) C38 – H112	1,20
	BD(2) C160 – O161	BD*(1) C58 – H130	1,67

From Table 1 it can be observed the presence of one the hydrogen bond formed between the ligands and the βCD, which in the case of the C1 ligand is formed between its H128 and the O22 of the βCD, while in C2 it is formed between its H168 and the O29 of the βCD, finally, in C3 it is formed between H167 and the O22 of the βCD.

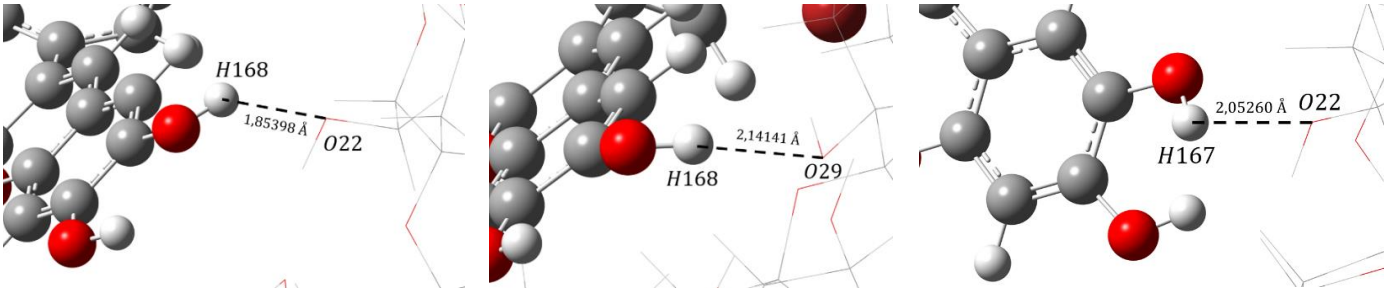

Figure 4. Hydrogen bond between coumarin-derived ligands and βCD cavity.

3.3 Thermodynamic parameters and non-covalent interactions (NCI)

The thermodynamic parameters allow describing the stability of the inclusion complexes, in turn, they allow describing the non-covalent interactions that stabilize the ligands in the βCD cavity, which are mainly van der Waals interactions and hydrogen bridges.

The thermodynamic parameters that guide the inclusion process of a ligand are the interaction energy [15,16], Gibbs free energy (ΔG°), enthalpy (ΔH°) and entropy (ΔS°) of reaction [11,12,13], which are described by the following equations and visualized in Table 2.

$$L + \beta CD \longrightarrow L/\beta CD \quad (1)$$

$$\Delta E_{int} = E_{L/\beta CD} - \left(E_L + E_{\beta CD}\right) + BSSE \quad (2)$$

$$\Delta G° = G^{\circ}_{L/\beta CD} - \left(G^{\circ}_{L} + G^{\circ}_{\beta CD}\right) \quad (3)$$

$$\Delta H° = H^{\circ}_{L/\beta CD} - \left(H^{\circ}_{L} + H^{\circ}_{\beta CD}\right) \quad (4)$$

$$\Delta S° = (\Delta H° - \Delta G°)/T \quad (5)$$

Table 2. Thermodynamic parameters of coumarin/βCD inclusion complex.

Thermodynamic parameters	βCD/C1	βCD/C2	βCD/C3
ΔE_{int} / $(kcal/mol)$	-17,67	-2,51	-9,52
ΔH° / $(kcal/mol)$	-145,35	-120,20	-138,23
ΔG° / $(kcal/mol)$	206,48	250,75	232,13
ΔS° / $(kcal/molK)$	-1,18	-1,24	-1,24

Table 2 shows that the inclusion complexes are energetically stable when presenting negative interaction energies ($\Delta E_{int} < 0$), since the more negative values, the more stable and favorable is the formation of the inclusion complex [47]. Therefore, the most stable complex is the βCD/C1, while the least stable is the βCD/C2.

Thermodynamically, Table 2 indicates that the gas-phase complexation process releases energy ($\Delta H^{\circ} < 0$) and is not spontaneous ($\Delta G^{\circ} > 0$) under normal pressure and temperature conditions (1 atm and 298 K). The negative enthalpy values describe the non-covalent interactions generated in the cavity of the complex, which are of the van der Waals and hydrogen bridging type. On the other hand, the negative entropy values ($\Delta S^{\circ} < 0$) describe the limitation of rotational and translational motion of the ligand in the cavity [15]. Therefore, the complexation of coumarin-derived ligands in βCD are mainly guided by enthalpy.

Non-covalent interactions (NCI) can be visualized through electron density analysis modeled with Multiwfn software and visualized in VMD, which models the interactions as color clouds, which are differentiated into strong interactions (hydrogen bonds) with a blue color, van der Waals-type interactions with a green color, and repulsive interactions with a red color [37]. The NCI analysis of the complexes can be seen in Figure 5.

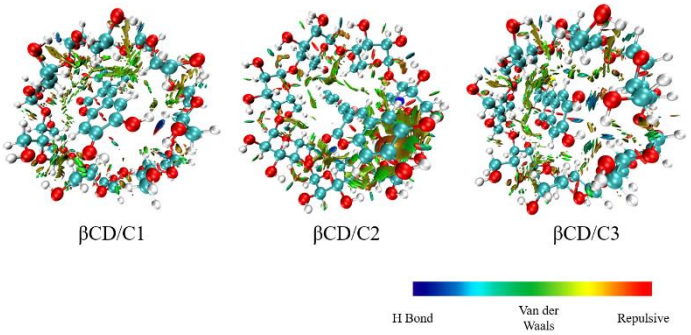

Figure 1. Non-covalent interactions generated in the cavity of the βCD inclusion complex with coumarin derivatives.

3.4 Global and local reactivity indices of ligands and inclusion complexes

From the theory of frontier molecular orbitals and Fleming's theory of reactivity [48], some quantities of chemical interest can be derived, such as the global and local reactivity indices [49]. Among the global reactivity indices are the chemical potential (μ) and electronegativity (χ) [50,51], the chemical hardness (η) and the electrophilicity index (ω) [26]. The local reactivity indices, on the other hand, are the Fukui functions ($f_{(r)}$) [27] and the dual descriptor ($f^{(2)}$) [28]. All global and local reactivity indices were calculated from the following equations, with their numerical values in Table 3.

$$\mu = \left(\frac{\partial E}{\partial N}\right)_{v_{(r)}} = \frac{1}{2}(\varepsilon_{LUMO} + \varepsilon_{HOMO}) \;;\; \chi = -\left(\frac{\partial E}{\partial N}\right)_{v_{(r)}} = -\frac{1}{2}(\varepsilon_{LUMO} + \varepsilon_{HOMO}) \quad (1)$$

$$\eta = \left(\frac{\partial \mu}{\partial N}\right)_{v_{(r)}} = \frac{1}{2}(\varepsilon_{LUMO} - \varepsilon_{HOMO}) \quad (2)$$

$$\omega = \frac{\mu^2}{2\eta} \quad (3)$$

$$f^{+}_{(r)} = \left(\frac{\partial \rho_{(r)}}{\partial N}\right)^{+}_{v_{(r)}} \approx \left|\psi_{(r)\,\mathrm{LUMO}}\right|^2 = \rho_{(r)\,\mathrm{LUMO}} \quad (4)$$

$$f^{-}_{(r)} = \left(\frac{\partial \rho_{(r)}}{\partial N}\right)^{-}_{v_{(r)}} \approx \left|\psi_{(r)\,\mathrm{HOMO}}\right|^2 = \rho_{(r)\,\mathrm{HOMO}} \quad (5)$$

$$f^{(2)}_{(r)} = \left(\frac{\partial f_{(r)}}{\partial N}\right)_{v_{(r)}} \approx f^{+}_{(r)} - f^{-}_{(r)} = \rho_{(r)\,\mathrm{LUMO}} - \rho_{(r)\,\mathrm{HOMO}} \quad (6)$$

Table 2. Global and local reactivity indices (×100) obtained through ONIOM2 (DFT/PM6) methods with the WB97XD/6-31G+(d,p) functional.

Especie	Átomo	$f^{-}_{(r)}$	$f^{+}_{(r)}$	$f^{0}_{(r)}$	$f^{(2)}_{(r)}$	μ / eV	η / eV	ω / eV
C1	4(C)	12,84	1,44	7,14	-11,40	-4,2741	7,3623	1,2306
	10(O)	10,12	0,60	5,36	-9,52			
	12(H)	0,25	0,07	0,16	-0,18			
	20(C)	3,31	0,16	1,73	-3,15			
	21(C)	6,34	10,12	8,23	3,78			
	26(O)	1,96	0,06	1,01	-1,90			
	27(O)	2,80	1,52	2,16	-1,28			
	29(H)	0,02	0,00	0,01	-0,02			
	30(H)	0,02	0,02	0,02	0,00			
βCD/C1	151(C)	16,82	1,16	8,99	-15,65	-5,6099	7,229	2,1767
	169(O)	11,30	0,13	5,71	-11,17			
	170(H)	0,16	0,05	0,10	-0,11			
	163(C)	2,38	13,23	7,80	10,85			
	164(C)	1,73	0,98	1,36	-0,75			
	165(O)	1,05	1,49	1,27	0,44			
	167(O)	0,61	0,09	0,35	-0,52			
	166(H)	0,01	0,04	0,02	0,03			
	168(H)	0,01	0,02	0,02	0,01			
C2	19(C)	10,42	0,09	5,25	-10,33	-4,2604	7,5291	1,2054
	20(C)	11,93	9,90	10,92	-2,03			
	24(O)	6,64	0,04	3,34	-6,60			
	26(O)	5,34	1,47	3,40	-3,88			
	28(H)	0,05	0,00	0,03	-0,05			
	29(H)	0,04	0,02	0,03	-0,02			
βCD/C2	163(C)	10,82	12,73	11,78	1,91	-5,7363	7,8845	2,0867
	164(C)	18,98	1,00	9,99	-17,97			
	165(O)	7,06	1,55	4,30	-5,51			
	167(O)	6,53	0,06	3,30	-6,46			
	166(H)	0,01	0,00	0,01	-0,01			
	168(H)	0,36	0,04	0,20	-0,32			
C3	16(C)	5,04	0,12	2,58	-4,92	-4,114	7,1177	1,1889
	17(C)	9,29	9,04	9,17	-0,25			
	21(O)	2,79	0,04	1,42	-2,76			
	22(O)	3,90	1,35	2,63	-2,56			
	25(H)	0,20	0,00	0,01	-0,02			
	26(H)	0,30	0,02	0,03	-0,01			
βCD/C3	162(C)	5,70	13,38	9,54	7,68	-5,6077	7,3694	2,1336
	163(C)	4,11	0,11	2,11	-4,00			
	166(O)	1,39	0,01	0,70	-1,38			
	164(O)	1,98	1,21	1,59	-0,77			
	167(H)	0,03	0,00	0,01	-0,03			
	165(H)	0,03	0,09	0,06	0,06			

In Table 3 it can be observed that the global descriptor that presents a lower variation with respect to the ligand and the inclusion complex is the chemical hardness, which can be understood as the resistance to electron density transfer, so it can be considered as a reactivity criterion, specifically if the "maximum hardness principle" (MHP) [52] is used, which describes that the most reactive systems have a low hardness, and the less reactive systems have a high hardness. Therefore, based on the MHP criterion, it can be observed that the C1 ligand has a higher reactivity in the inclusion complex, while the C2 and C3 ligands decrease their overall reactivity.

In Table 3 it can be observed that the global descriptor that presents a lower variation with respect to the ligand and the inclusion complex is the chemical hardness, which can be understood as the resistance to electron density transfer, so it can be considered as a reactivity criterion, specifically if the "maximum hardness principle" (MHP) [52] is used, which describes that the most reactive systems have a low hardness, and the less reactive systems have a high hardness. Therefore, based on the MHP criterion, it can be observed that the C1 ligand has a higher reactivity in the inclusion complex, while the C2 and C3 ligands decrease their overall reactivity.

Electrophilicity is a measure of "electrophilic power" or the ability of a chemical species to attract electron density and how this stabilizes the system [25], so that an increase in the electrophilicity indexes of all the ligands in the inclusion complex can be observed, translating this parameter into a criterion of stability [36] and electrophilic capacity, with the C1 ligand having the highest electrophilic power (1.2306 eV and 2.1767 eV).

In the same way, it can be observed from the chemical potential, specifically the negative value of this (eq. 7), that the tendency of attracting electron density is consistent with the Electrophilicity values, being a parameter that is also able to describe the antioxidant capacity by SET mechanism [21,23,24,25,26]. The electronegativity values increase in each ligand when the inclusion complex is formed (as well as the Electrophilicity), being C1 the one with the highest electronegativity value.

For antioxidant compounds that have hydroxyl groups in their structure (such as substituted polyphenols and flavonoids), the atoms of interest are the hydrogens and oxygen of the hydroxyl group, and the carbon atoms containing these groups. From Table 3, the electrophilic and nucleophilic tendencies of an atom can be identified according to the values of the Fukui functions and the dual

descriptor, with large values of $f_{(r)}^{+}$ being susceptible sites to nucleophilic attacks, while large values of $f_{(r)}^{-}$ are sites susceptible to electrophilic attacks [27]. In turn, when the dual descriptor values are $f_{(r)}^{(2)} > 0$ they represent sites prone to nucleophilic attacks, while values of $f_{(r)}^{(2)} < 0$ describe sites prone to electrophilic attacks [28].

From Table 3 it can be observed that the carbon atoms in the C1 ligand present a behavior susceptible to electrophilic and nucleophilic attacks, being the 4(C) and 20(C) those who present high values of $f_{(r)}^{-}$ and negative values of $f_{(r)}^{(2)}$. While 21(C) presents high values of $f_{(r)}^{+}$ and positive values of $f_{(r)}^{(2)}$. On the other hand, all the oxygens present an electrophilic tendency by presenting high values of $f_{(r)}^{-}$ and negative values of $f_{(r)}^{(2)}$. This behavior of chemical reactivity of the carbon and oxygen atoms is maintained in the inclusion complex, except for 20(C), 21(C) and 26(O) which change their characteristics from electrophilic to nucleophilic tendencies, and vice versa.

The behavior of the hydrogen atoms is perhaps the most important, since they are the ones that perform the AOX HAT mechanism [22], so from Table 5 it can be observed that the C1 and C3 ligands do not present AOX HAT capacity in situ, since their hydrogens present negative values of $f_{(r)}^{(2)}$, which change in the inclusion complex, specifically hydrogens 29(H) and 30(H) (166(H) and 168(H) in the complex) of C1, and 26(H) (165(H)) of C3, presenting positive values of $f_{(r)}^{(2)}$ which confers an electroacceptor characteristic, or, the characteristic of "labile hydrogen", which can be easily yielded through a radical cleavage towards the free radical.

A theoretical/experimental study [53] describes the AOX reactivity through the radical Fukui indices ($f_{(r)}^{0}$) of the oxygen atoms of the hydroxyl groups. According to a higher value of $f_{(r)}^{0}$ this molecular segment presents a higher antioxidant activity, so for the coumarinic ligand C1 it can be observed that it presents a higher value of $f_{(r)}^{0}$ in the position 10(O) and in the same position inside the inclusion complex (169(O)), presenting a slight increase in its value, so the ligand inside the cavity of the inclusion complex describes a change in its reactivity, in the same way as the ligands C2 and C3.

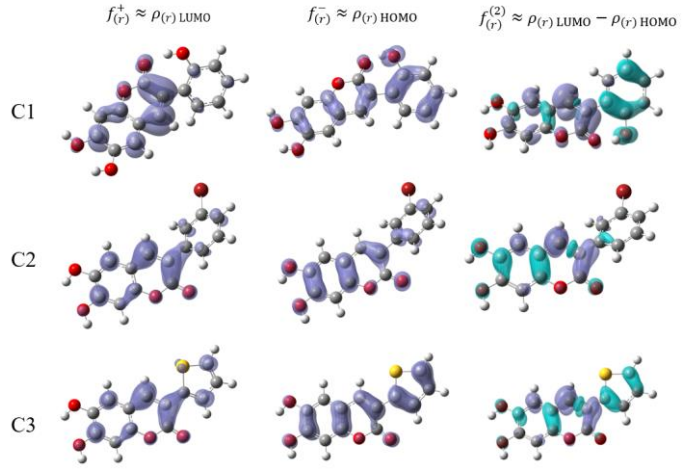

Figure 6. Local descriptors of coumarin-derived ligand reactivity.

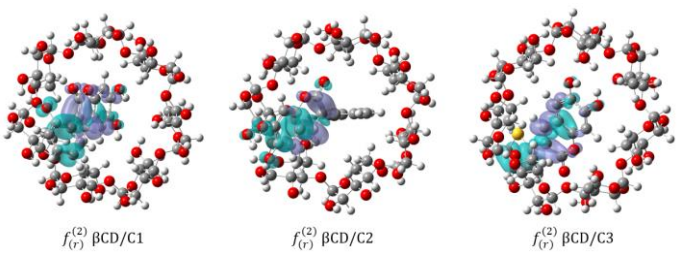

Figure 7. Dual descriptor of coumarin-derived ligands in complex with βCD.

CONCLUSION

According to the thermodynamic and reactivity results, it can be concluded that the coumarin-derived ligands change their reactivity and are able to form stable inclusion complexes with βCD, which are stabilized by non-covalent van der Waals-type interactions and hydrogen bond. The thermodynamic parameters show that the complexation is not spontaneous under the modeling conditions (gas phase and normal conditions of pressure and temperature), but it does demonstrate the stability and viability of the complexes by presenting interaction energy and negative enthalpy, which guides the complexation process.

The chemical reactivity modeled through global and local descriptors indicates that the coumarin derivatives change their reactivity *in situ* and in the cavity of the inclusion complex, in addition it can be observed that these ligands present variable antioxidant activity as it can be by SET and HAT mechanisms.

CONFLICT OF INTEREST

The authors have no conflicts of interest to declare.

ACKNOWLEDGMENTS

Grateful for the PIDi - UTEM high performance computing system (SCC - PIDi - UTEM CONICYT - FONDEQUIP - EQM180180) of the Universidad Tecnológica Metropolitana, Santiago, Chile, for providing the computational support to perform the computational calculations. Thanks to Dr. Claudio Olea (Universidad de Chile) and Dr. Lucia Otero (Universidad de la Republica de Uruguay) for providing the coumarin ligands for the study.

REFERENCES

1. Lin, Yuheng, Sun, Xinxiao, Yuan, Qipeng; Yan, Yajun. combinatorial biosynthesis of plant-specific coumarins in bacteria. Metabolic Engineering., 18(0), 69 – 77. (2013).
2. G. Kirsch, A. Abdelwahab, P. Chaimbault, Natural and Synthetic Coumarins with Effects on Inflammation. Molecules, 21(10), 1322. (2016)
3. I.Kostova, S. Bhatia, P. Grigorov, S. Balkansky, S. Parmar, V. K. Prasad, & L. Saso. Coumarins as Antioxidants. Current Medicinal Chemistry, 18(25), 3929–3951. (2011)
4. T. Verhoef, W. Redekop, A. Daly, R. van Schie, A. de Boer, A. Maitland-van der Zee. Pharmacogenetic-guided dosing of coumarin anticoagulants: algorithms for warfarin, acenocoumarol and phenprocoumon. British Journal of Clinical Pharmacology, 77(4), 626–641. (2014)
5. F. Pérez-Cruz, S. Serra, G., Delogu, M. lapier, J. Maya, C. Olea-Azar, Santana, E. Uriarte. antitrypanosomal and antioxidant properties of 4-hydroxycoumarins derivatives. bioorganic & medicinal chemistry letters, 22(17), 5569 – 5573. (2012)
6. J. Szejtli. Past, present and future of cyclodextrin research. Pure and Applied Chemistry, 76(10), 1825–1845. (2004)
7. T. Loftsson, D. Duchene. Cyclodextrins and their pharmaceutical applications. International Journal of Pharmaceutics, 329(1-2), 1–11. (2007)
8. C. Grégori. Review: A History of Cyclodextrines. Chemical Review, 114 (21), 10940 – 10975. (2014)
9. K. Connors. The Stability of Cyclodextrin Complexes in Solution. Chemical Reviews, 97(5), 1325–1358. (1997).
10. A.Radi, S. Eissa. Electrochemistry of cyclodextrin inclusion complexes of pharmaceutical compounds. Open Chemical and Biomedical Methods Journal, 3, 74 – 85. (2010)
11. M. R. Nora, L. Ismahan, G. Abdelkrim, C. Mouna, N. Leila, M. Fatiha, B. Nada, H. Brahim. Interactions in inclusion complex of β-cyclodextrin/l-Metheonine: DFT computational studies. Journal of Inclusion Phenomena and Macrocyclic Chemistry, 96, 43 – 54. (2019)
12. S. K. Xing, C. Zhang, H. Ai, Q. Zhao, Q. Zhang, D. Sun. Theoretical study of the interactions of β-cyclodextrin with 2′-hydroxyl-5′-methoxyacetophone and two of its isomers. Journal of Molecular Liquids, 146(1-2), 15 – 22. (2009)
13. F. D'Aria, B. Pagano, C. Giancola. Thermodynamic properties of hydroxypropyl-β-cyclodextrin/guest interaction: a survey of recent studies. Journal of Thermal Analysis and Calorimetry. (2021)
14. P.D. Ross, M. V. Rekharsky. Thermodynamics of hydrogen bond and hydrophobic interactions in cyclodextrin complexes. Biophysical Journal, 71(4), 2144 – 2154. (1996)
15. Á. Vidal Vidal, L. de Vicente Poutás, O. Nieto Faza, C.S. López. On the Use of Popular Basis Sets: Impact of the Intramolecular Basis Set Superposition Error. Molecules, 24(20), 3810. (2019)

16. F. B. Van Duijneveldt, J. G. van Duijneveldt-van de Rijdt, J. H. van Lenthe. State of the Art in Counterpoise Theory. Chemical Reviews, 94(7), 1873 – 1885. (1994)
17. A.Reed, L. Curtiss, F. Weinhold. Intermolecular interactions from a natural bond orbital, Donor – acceptor viewpoint. Chemical Reviews, 88(6), 899 – 926. (1988)
18. B.D. Dunnington, J. R. Schmidt, J. R. Generalization of Natural Bond Orbital Analysis to Periodic Systems: Applications to Solids and Surfaces via Plane-Wave Density Functional Theory. Journal of Chemical Theory and Computation, 8(6), 1902–1911. (2012)
19. E.D. Glendening, C.R. Landis, F. Weinhold. Natural bond orbital methods. Wiley Interdisciplinary Reviews: Computational Molecular Science, 2(1), 1 – 42. (2011)
20. T. Lu, & F. Chen. Multiwfn: A multifunctional wavefunction analyzer. Journal of Computational Chemistry, 33(5), 580–592. (2011)
21. M. Farrokhnia. Density Functional Theory Studies on the Antioxidant Mechanism and Electronic Properties of Some Bioactive Marine Meroterpenoids: Sargahydroquionic Acid and Sargachromanol. ACS omega, 5(32), 20382–20390. (2020)
22. V.K. Rajan, K. Muraleedharan. A computational investigation on the structure, global parameters and antioxidant capacity of a polyphenol, Gallic acid. Food Chemistry, 220, 93 – 99. (2017)
23. L.C. Balbás, J.A. Alonso, L.A. Vega. Density functional theory of the chemical potential of atoms and its relation to electrostatic potentials and bonding distances. Z Phys D - Atoms, Molecules and Clusters 1, 215–221 (1986)
24. S. Figueredo, M. Páez, F. Torres. índices de poder electrofílico global y local para el estudio teórico de la reactividad química: aplicación a derivados carbonilo α, β-insaturados. Química Nova, 40(5), 513 – 522. (2017)
25. V.P. Gupta. Characterization of Chemical Reactions. Principles and Applications of Quantum Chemistry, 385–433. (2016)
26. R.G. Parr, L. Szentpály, S. Liu. Electrophilicity Index. Journal of the American Chemical Society, 121(9), 1922–1924. (1999)
27. R.G. Parr, W. Yang. Density Functional Approach to the Frontier - Electron Theory of Chemical Reactivity, Journal of the American Chemical Society 106. 4049 – 4050. (1984)
28. C. Morell, A. Grand, A. Toro-Labbé. New dual descriptor for chemical reactivity. Journal of Physical Chemistry A 109, 205–212. (2005)
29. M. J. Frisch, G. W. Trucks, H. B. Schlegel, G. E. Scuseria, M. A. Robb, J. R. Cheeseman, G. Scalmani, V. Barone, B. Mennucci, G. A. Petersson, H. Nakatsuji, M. Caricato, X. Li, H. P. Hratchian, A. F. Izmaylov, J. Bloino, G. Zheng, J. L. Sonnenberg, M. Hada, M. Ehara, K. Toyota, R. Fukuda, J. Hasegawa, M. Ishida, T. Nakajima, Y. Honda, O. Kitao, H. Nakai, T. Vreven, J. A. Montgomery, Jr., J. E. Peralta, F. Ogliaro, M. Bearpark, J. J. Heyd, E. Brothers, K. N. Kudin, V. N. Staroverov, R. Kobayashi, J. Normand, K. Raghavachari, A. Rendell, J. C. Burant, S. S. Iyengar, J. Tomasi, M. Cossi, N. Rega, J. M. Millam, M. Klene, J. E. Knox, J. B. Cross, V. Bakken, C. Adamo, J. Jaramillo, R. Gomperts, R. E. Stratmann, O. Yazyev, A. J. Austin, R. Cammi, C. Pomelli, J. W. Ochterski, R. L. Martin, K. Morokuma, V. G. Zakrzewski, G. A. Voth, P. Salvador, J. J. Dannenberg, S. Dapprich, A. D. Daniels, Ö. Farkas, J. B. Foresman, J. V. Ortiz, J. Cioslowski, and D. J. Fox, Gaussian 09, Revision E. 01, Gaussian, Inc., Wallingford CT. (2013)
30. J.D. Chai, M. Head-Gordon. Long-range corrected hybrid density functionals with damped atom–atom dispersion corrections. Physical Chemistry Chemical Physics, 10(44), 6615. (2008)
31. M. Adachi, B. Mikami, T. Katsube, S. Utsumi. Crystal Structure of Recombinant Soybean β-Amylase Complexed with β-Cyclodextrin. Journal of Biological Chemistry, 273(31), 19859 – 19865. (1998)
32. G.M. Morris, R. Huey, W. Lindstrom, M.F. Sanner, R.K. Belew, D.S. Goodsell, A.J. Olson. AutoDock4 and AutoDockTools4: Automated docking with selective receptor flexibility. Journal of Computational Chemistry, 30(16), 2785 – 2791. (2009)
33. E. Faúndez. Efecto de dimetil – β – ciclodextrina en la interacción de moléculas heterocíclicas con ADN y metales de transición de importancia biológica. Repositorio Universidad de Chile. Facultad de Ciencias Químicas y Farmaceuticas. (2016)
34. L.W. Chung, W.M.C. Sameera, R. Ramozzi, A.J. Page, M. Hatanaka, G.P. Petrova, K. Morokuma. The ONIOM Method and Its Applications. Chemical Reviews, 115(12), 5678–5796. (2015)
35. E. Glendening, J. Badenhoop, A. Reed, J. Carpenter, C. Bohmann, C. Morales, C. Landis, F. Weinhold. NBO 6.0: Natural Bond Orbital analysis program. Journal of Computational Chemistry, 34(16), 1429 – 1437. (2013)
36. K. Sahra, K. Dinar, A. Seridi, M. Kadri. Investigation on the inclusion of diclofenac with β-cyclodextrin: a molecular modeling approach. Structural Chemistry, 26(1), 61 – 69. (2015)
37. W. Humphrey, A. Dalke, K. Schulten. "VMD - Visual Molecular Dynamics", Journal of Molecular Graphics, 14, 33 – 38. (1996)
38. R. Contreras, P. Fuentealba, M. Galván, P. Pérez. Chemical Physical Letters. 304(5-6), 405-413. (1999)
39. P. Fuentealba, P. Pérez, R. Contreras. Journal of Chemical Physics 113(7), 2544-2551. (2000)
40. S. Y. Huang, X. Zou, X. Advances and Challenges in Protein-Ligand Docking. International Journal of Molecular Sciences, 11(8), 3016 – 3034. (2010)
41. L. Ismahan, N. Leila, M. Fatiha, G. Abdelkrim, C. Mouna, B. Nada, H. Brahim, H. Computational study of inclusion complex of l-Glutamine/beta-Cyclodextrin: Electronic and intermolecular interactions investigations. Journal of Molecular Structure, 127740. (2020)
42. M.E. Davis, M.E. Brewster. Cyclodextrin-based pharmaceutics: past, present and future. Nature Reviews Drug Discovery, 3(12), 1023 – 1035. (2004)
43. T. Li, R. Guo, Q. Zong, G. Ling. Application of molecular docking in elaborating molecular mechanisms and interactions of supramolecular cyclodextrin. Carbohydrate Polymers, 118644. (2021)
44. P.D. Ross, M.V. Rekharsky. Thermodynamics of hydrogen bond and hydrophobic interactions in cyclodextrin complexes. Biophysical Journal, 71(4), 2144 – 2154. (1996)
45. M.V. Rekharsky, Y. Inoue. Complexation thermodynamics of cyclodextrins. Chemical reviews, 98(5), 1875 – 1918. (1998)
46. F. Biedermann, W.M. Nau, H.J. Schneider. The Hydrophobic Effect Revisited – Studies with Supramolecular Complexes Imply High – Energy Water as a Noncovalent Driving Force. Angewandte Chemie International Edition, 53(42):11158 – 11171. (2014)
47. A.Fifere, N. Marangoci, S. Maier, A. Coroaba, D. Maftei, M. Pinteala. Theoretical study on β-cyclodextrin inclusion complexes with propiconazole and protonated propiconazole. Beilstein Journal of Organic Chemistry, 8, 2191–2201. (2012)
48. Fleming. Orbitales moleculares y reacciones de química orgánica. 1era Edición. Editorial Wiley. Cap. 3. pp. 127 – 143. (2010)
49. R. Parr, W. Yang. Density - Functional Theory of Atoms and Molecules, Chapter 4. Oxford University Press: New York. Ca. (1989)
50. R. Parr, R. Donnelly, M. Levy, W. Palke. Electronegativity: the density functional viewpoint. Journal of Chemical Physical, 68, 3801. (1978)
51. R.P. Iczkowski, J. L. Margrave. Electronegativity. Journal of the American Chemical Society, 83(17), 3547 – 3551. (1961)
52. R.G. Pearson. Chemical Hardness: Aplications from Molecules to Solids, Wiley-VCH Verlag GMBH: Weinheim. Chapter 4. pp. 99-124. (1997)
53. K. Pérez-Cruz, M. Moncada - Basualto, J. Morales-Valenzuela, G. Barriga - González, P. Navarrete-Encina, L. Núñez - Vergara, J.A. Squella, C. Olea-Azar. Synthesis and antioxidant study of new polyphenolic hybrid - coumarins. Arabian Journal of Chemistry, 11(4), 525–537. (2018)